



HAL
open science

Epileptic transient detection: wavelets and time-frequency approaches.

Lotfi Senhadji, Fabrice Wendling

► **To cite this version:**

Lotfi Senhadji, Fabrice Wendling. Epileptic transient detection: wavelets and time-frequency approaches.. Neurophysiologie Clinique = Clinical Neurophysiology, 2002, 32 (3), pp.175-92. <10.1016/S0987-7053(02)00304-0>. <inserm-00130050>

HAL Id: inserm-00130050

<https://inserm.hal.science/inserm-00130050v1>

Submitted on 15 Feb 2007

HAL is a multi-disciplinary open access archive for the deposit and dissemination of scientific research documents, whether they are published or not. The documents may come from teaching and research institutions in France or abroad, or from public or private research centers.

L'archive ouverte pluridisciplinaire **HAL**, est destinée au dépôt et à la diffusion de documents scientifiques de niveau recherche, publiés ou non, émanant des établissements d'enseignement et de recherche français ou étrangers, des laboratoires publics ou privés.



HAL Authorization

Epileptic Transient Detection : Wavelets and Time-Frequency Approaches

Lotfi Senhadji, Fabrice Wendling

Laboratoire Traitement du Signal et de l'Image

EM-INSERM 9934, Université de Rennes 1

Rennes, 35042 Cedex, France.

Lotfi.Senhadji@univ-rennes1.fr**1 Introduction**

The extraction of useful information, conveyed by a given signal, is of major importance in the understanding of underlying mechanisms and for the elaboration of decisions and actions. Any system dedicated to this task leans on a step of analysis of information contents.

When dealing with time-series signals, the analysis of their evolution in the direct space of representation, is classically complemented by the examination of an equivalent representation in the Fourier domain. Although, these two representations allow characteristics of signals to be globally extracted, they can appear insufficient or even unsuitable for the analysis of local properties. Indeed, by switching to the Fourier domain, a mathematically equivalent representation is obtained but all the explicit temporal descriptions of the signal are lost. If this dual aspect of Fourier's representation has no consequence on signals stemming from a linear or a time-invariant system, it is a major drawback when the purpose is to analyze the spectral contents of a signal on a variable window length.

Several representations allying time and frequency or time and scale of analysis were introduced in literature. They can be either linear or nonlinear, parametric or not parametric, complete or incomplete, etc. . Each of these representations describes the signal by highlighting some of its characteristics while the others are relegated in the background. Therefore the choice of a representation is crucial and influences the post-processing outcomes.

In a given context, the useful information carried by a signal can be related to its almost stable or slowly evolutionary dynamics, to the occurrence of abrupt ruptures or transients but also to the chronologies of these events. The main part of the conveyed information appeared then as *nonstationarities* on the signal. A signal is assumed to be stationary if its statistical properties (mean, variance, autocorrelation, ...) are invariant over time. Fourier representation is particularly adapted for the description of stationary signals. Such a signal can exhibit unexpected events but their probabilities are known. There is a wide range of nonstationary signals. Depending on the type of encountered nonstationarities (transient events, frequency modulation, ...), a specific analysis technique is required. Therefore, describing nonstationary signals is generally difficult since there exists no universal or canonical tool to achieve this task.

Among methods aimed at analyzing nonstationary signals, time-scale and time-frequency approaches have been extensively used during the last decade. The ability of these methods to address some key issues for representing nonstationary signals gave rise to new insights and fruitful multidisciplinary developments. Thus, writing a self-contained and complete overview of time-scale and time-frequency approaches and their applications is not

the intent of the present article. Subsequent published materials (papers, books, special journals, ...) highlighting these issues are then recommended (1-19).

Time-scale representations or “wavelets analysis” offer a time versus duration analysis of the observed phenomenon. Hence, they allow to focus on short events and to characterize them by means of their evolution throughout the set of analysis scales. The use of wavelet approaches for studying transient signals is then rational. Time-frequency approaches permit the description, according to time and frequency, of the evolution of the signal energy distribution. They allow time-frequency structures or signatures that characterize the dynamics of the observed signal to be extracted. It is then natural to consider these methods for the analysis of signals for which the energy distributions vary gradually over time.

Electroencephalographic signals (EEG), as most of biomedical signals, are nonstationary and these nonstationarities often contain significant information regarding the originating mechanisms and the underlying pathophysiological processes. Among available methods used in the investigation of epileptic patients, EEG keeps a high potential clinical value (20). EEG signals may be recorded from scalp electrodes (conventional EEG), from subdural electrodes (electrocorticography, ECoG) or from intracerebral electrodes usually implanted under stereotactic conditions (stereoelectroencephalography, SEEG) (21). Signal processing methods may bring substantial complement to visual analysis of EEG signals, especially during epileptic episodes (both ictal and interictal periods) where signals often exhibit nonstationary properties.

In this context, time-scale and time-frequency methods, introduced in the field of epileptic EEG about ten years ago, were shown to provide meaningful representations of isolated events, as spikes, spike-waves, sharp-waves (22) and of the complex evolution of signal spectral content as a function of time during ictal periods (23).

The aim of the current paper is to give a didactic overview of both wavelets and time-frequency methods, and their potential contribution to the description of the epileptic electroencephalography is illustrated in two examples : the first one deals with interictal events detection on scalp EEG ; the second one is aimed at classifying depth-EEG signatures. The following section presents the theoretical background of wavelet transforms and its application for spikes detection. In section 3, time-frequency representations are introduced and their potential use for extracting particular signatures in SEEG is investigated. Concluding remarks are reported in section 4.

2 Wavelet Transform

From the conceptual point of view, the wavelet transform (WT) is not new. It consists of representing a signal S by means of a linear combination of elementary functions. The same idea is used in the Fourier transform where the elementary functions are sinusoids. One of the originalities of WT is the set \mathcal{F} of elementary or decomposing functions which are obtained after scaling (dilating) and translating a unique function denoted ψ , called wavelet, and verifying some admissibility conditions (24).

2.1 Wavelets Theoretical background

The coefficients or details resulting from the WT are denoted $WT_s(a, t; \psi)$ with :

$$WT_s(a, t; \psi) = \frac{1}{\sqrt{|a|}} \int_{-\infty}^{+\infty} S(u) \psi_{a,t}^*(u) du$$

where * designates the complex conjugate, and :

$$\mathcal{F} = \left\{ \psi_{a,t} \in L^2(\mathbb{R}) / \psi_{a,t}(u) = \frac{1}{\sqrt{|a|}} \psi\left(\frac{u-t}{a}\right), a \neq 0, t \in \mathbb{R} \right\}$$

For a and t continuously varying (a nonzero and t real), the set of $WT_S(a, t; \psi)$ constitutes the (*continuous*) *wavelet transform*. Parameter a is the scaling factor, used both to control the time duration of the wavelet and to ensure the normalization of its energy that must be equal to 1. Parameter t is the translation factor, used to position the wavelet over the axis u which is the time axis in temporal signal analysis. Wavelet transform can be interpreted as a filtering

process of signal S . In fact, by defining $\tilde{\psi}_a(u) = \frac{1}{\sqrt{|a|}} \psi^*\left(\frac{-u}{a}\right)$, $WT(a, t; \psi)$ can be written as

:

$$WT_S(a, t; \psi) = \int_{-\infty}^{+\infty} S(u) \tilde{\psi}_a(t-u) du$$

This last equation shows that $WT_S(a, t; \psi)$ is the output, observed at time t , of a filter whose impulse response is given by the function $\tilde{\psi}_a$, where the scale a is used to adjust the bandwidth (i.e. the frequency resolution), and S being the input. Thus, this transformation acts on the signal as a filter bank whose frequency characteristics are related to the analyzing wavelet ψ and to the dilation factor a .

The admissibility conditions wavelets must satisfy are rather weak. Therefore, many wavelet transforms may be defined. For a given purpose, this allows an analyzing wavelet tailored to match the signal characteristics to be delineated and parameters a and t to be freely selected without constraining them to any particular value. In other words, from *a priori* knowledge about the signal, the analysis may be restricted to an appropriate set of scaling parameters.

Generally, under these only conditions, the set \mathcal{F} does not provide a basis of $L^2(\mathbb{R})$ ¹ and the resulting transform is thus redundant : the signal, which is initially a one dimensional function of time, is mapped into an equivalent two dimensional image, which axes are the time t and the scale a , while the amount of conveyed information remains unchanged (only its representation is modified). In figure 1, an academic case is reported to illustrate the gain that might be expected when changing the representation domain. The considered signal, in the left panel, is the sum of two transients having the same shape but different durations. The right panel, corresponding to a continuous wavelet representation of the signal, clearly outlines the ability of wavelet transform to describe efficiently the signal : two signatures are revealed in the wavelet domain, corresponding to the transient components of the signal.

When specific mathematical properties are verified, both on the analyzing wavelets ψ and on the set of dilations and translations parameters, an orthonormal wavelet basis of $L^2(\mathbb{R})$ can be derived from \mathcal{F} . This leads to the *orthonormal wavelet transform* (OWT) (sometimes called *discrete wavelet transform-DWT*). Indeed, for particular wavelets and for the discrete grid given by the series $a = 2^{-m}$ (dyadic scales), $t = n.a$, where m and n are integers, the associated subset of \mathcal{F} constitutes an orthonormal basis of $L^2(\mathbb{R})$ (25). The wavelet analysis is thus seen through the associated multiresolution analysis (or filter bank) and the decomposition over an orthogonal basis of $L^2(\mathbb{R})$ leads to a cascade of high-pass and low-pass filtering of the signal followed by decimations. The signal S is then decomposed into a discrete set of orthogonal details ensuring the exact reconstruction of the original signal (26).

¹ The set of functions of finite energy

Intermediate situations do exist. For example, *biorthogonal wavelet transforms* use the same grid but impose less constraint on the wavelets used for decomposing and reconstructing the signal, *dyadic wavelet transforms* use the dyadic scales whereas the parameter t varies continuously over time. Readers interested in these aspects of wavelet analysis may refer to (10).

Then, for describing a signal, we have a multitude of wavelet transforms at hand. Consequently, the choice must be motivated by the seeking goals. Each representation has its own advantages and limitations : orthogonal and biorthogonal wavelet transforms are useful in the field of coding where the target is to compress the information and to reduce redundancies. They are less relevant for singularity detection and pattern recognition where properties like translation invariance and localization are desirable (27, 28). Dyadic or continuous wavelet transforms are indeed suitable for addressing such issues (29). These methods have been used in different areas of biomedical engineering. In this context, an overview of potential applications is given in (5, 18, 19).

2.2 Wavelet transform based interictal transient detection

The objective of this section is to illustrate the usefulness of WT through the problem of detection of interictal events, like spikes or spikes-waves. These transients are generally of short duration, they have imprecise shapes and are mixed to additive noise. For this class of signals, usual hypotheses (stationarity, gaussian assumption ...) are not verified and restrict, this way, the use of classical tools of analysis. As the relevant events are brief and occur in the signals as "details" or singularities, well localized in time, time-scale approaches offer a sound framework for their description. Figure 2 depicts the representation of a 10 seconds period of

a surface EEG recorded during interictal episodes on a patient suffering from a left temporal lobe epilepsy. The signal exhibits artifact transients activities, various background shapes and interictal events. Such a signal can be modeled, after sampling, by a random process $X(k)$ such that (30) :

$$X(k) = F(k) + \sum_{i=1}^{n_p} P_i(k - t_{p_i}) + \sum_{j=1}^{n_a} A_j(k - t_{a_j}) + B(k)$$

This relation expresses the relevant activities (elementary waves, background activity, noise, artifacts ...) which constitute the signal (see Figure 2). $F(k)$, the background activity, may be considered as a piece-wise stationary signal present either casually or over the whole duration of the observation; for each i , P_i represents a brief duration potential, occurring at the random time t_{p_i} , and corresponding to an abnormal neural discharge; the A_j terms may be related to artifacts occurring at unpredictable times t_{a_j} ; finally, measurement noise which are stationary over the observation duration are gathered in the term $B(k)$; the entities n_p and n_a respectively represent the unknown number of temporal occurrences of brief useful events and artifact transient signals over the observation period.

The component $F(k)$ includes basic activities (Alpha, Beta ...) as well as ictal stationary periods of time (recruitment phase during an epileptic seizure for example). The distinction between the A_j and P_i terms depends on the goals of the study : in our case, the epileptic events to be detected are described by the P_i terms ; conversely, transient waves associated to sleep, vertex sharp transients or K complexes belong to the set of artifacts. In all cases, and this, independently from the application, transient signals generated by eye movements are represented by A_j terms. Applying continuous wavelet transform to the derivation Fp2-F8

(Figure 3) allows interictal events to be enhanced over particular scales and thus open the way for their detection.

Based on the above remarks, we proposed, about ten years ago (30, 31), the first EEG interictal event detector using continuous wavelet transform. Briefly, a two level decision system was designed (Figure 4). The first stage is aimed at separating background activity and measurement noise from transient signals (useful transients and artifacts,). The decision structure is quadratic (to avoid phase variations sensitivity) and makes use of a filtering / squaring / summation scheme. At the output of the first detection level, the transient signals are enhanced when compared to the background activity (Figure 3) without a specific distinction between epileptic events and artifacts (mainly induced by muscular activity and eye movements). The crossing of a first threshold λ_1 allows to select the observation instants where an impulse-like signal occurs. Experimentally, when a significant wave or an artifact is present, the wavelet transform evolves through scales accordingly : the A_j are magnified on the smallest scales. The squared modulus increases (resp. decreases) for high resolution if the threshold crossing is due to an artifact (resp. useful wave) (32, 33). These considerations led us to build the second level. It is based on a decision parameter, derived from the wavelet domain representation. Separation between the useful transients and artifacts is then obtained by comparing this parameter to a second threshold λ_2 . Finally, threshold λ_1 is estimated for controlling the false alarm rate and threshold λ_2 is computed to guarantee a minimal rate of good classification of useful transients and artifacts.

2.3 *Remarks about WT and detection*

To our knowledge, this was the first wavelet based interictal event detector proposed in the literature. In the case of scalp EEG signals, performances of the above detector

HAL author manuscript inserm-00130050, version 1

compared favorably, in terms of sensitivity and specificity, to those of other detectors described elsewhere (34-36). It is now available on a digital EEG monitoring system². Such a detection methodology may be used as a building block into a general context based detection procedures of epileptic transients as those proposed in (37-40), Other detectors using wavelets have been proposed for detecting epileptic transients events : multiresolution analysis is proposed for the study of EEG in (41) and (42). Interictal spike detection strategies are proposed in (43-46) based on biorthogonal wavelet transforms as well as on continuous wavelet transform. WT has also been considered for seizure onset detection and characterization (42, 47).

Today, the main challenge is to make already developed wavelet methods available as tools for analyzing epileptic recordings in clinical context.

3 Time-Frequency representation

Rather than decomposing a signal S according to a given set of functions, Time-Frequency Representations (TFR) lean on a transformation which objective is to represent the signal energy distribution in the time-frequency domain. Several association rules, between the signal and the transformation, can be considered (6). Energy being a quadratic transformation of the signal, it is natural to pay particular attention to quadratic energy distribution representations.

3.1 Time-Frequency theoretical background

To obtain such a joint time and frequency distribution of energy, the concepts of instantaneous power $|S(t)|^2$ and power spectrum density $|\hat{S}(f)|^2$ are combined. If one

² Deltamed Co., Paris, France

considers that S belongs to $L^2(\mathbb{R})$, it is natural to look for a representation $T_s(t, f)$ as " joint energy density " such as its summation over the time-frequency plane allows recovering the signal energy.

It is important to note that $T_s(t, f) = \left| WT_s \left(\frac{1}{f}, t; \psi \right) \right|^2$ is a quadratic energetic time-frequency distribution and is known as the scalogram. It is however a very particular time-frequency distribution.

Among the various possible forms of $T_s(t, f)$ we focus in the following on the Cohen class of distributions. It gathers all time-frequency shift invariant, energetic, quadratic distributions (17). Any distribution of this class is given by :

$$T_s(t, f; \varphi) = \iiint \varphi(\tau, \nu) e^{j2\pi\nu(s-t)} S\left(s + \frac{\tau}{2}\right) S^*\left(s - \frac{\tau}{2}\right) e^{-j2\pi f\tau} d\nu ds d\tau$$

where S is the signal to be analyzed, τ , t , and s are temporal variables, f and ν frequency variables and φ is an arbitrary function, called kernel function. The characteristics of this kernel determine the properties of the associated TFR. The simplest kernel ($\varphi(\tau, \nu) = 1$) corresponds to the so-called Wigner-Ville Distribution (WVD), given by :

$$WVD_s(t, f) = \int S\left(t + \frac{\tau}{2}\right) S^*\left(t - \frac{\tau}{2}\right) e^{-j2\pi f\tau} d\tau$$

and which plays a fundamental role. Indeed, any distribution of the Cohen class can be written as a two-dimensional convolution between the WVD and the 2D Fourier transform of $\varphi(\tau, \nu)$.

The WVD has a very good resolution but suffers from the presence of interference terms related to the nonlinear character of the transformation. Although these terms are carrying information, they may limit the interpretation of the time-frequency representation. The interference terms are of oscillatory nature, they can then be attenuated by a smoothing (i.e. convolutions with a low-pass kernel) of the WVD. It should be noted that the attenuation of the interference terms comes with a degradation of the time and frequency resolutions. Many authors proposed particular low-pass kernels to reduce the interference terms while preserving, as much as possible, the resolution of the WVD and most of its properties. Readers interested by an overview on TFR can refer to (7, 17) or (48).

An academic example is considered in Figure 5 where two signals are analyzed. The first signal (top left panel) is the sum of 4 bursts : two of them have the same frequency but different time positions while the two others occur at the same time but have different frequencies. Its Wigner-Ville representation shows (middle left panel) 4 auto-terms and 6 cross-terms (two of them overlap) that correspond to the interaction between the signal components. The smoothing of the Wigner-Ville representation (bottom left panel) suppresses the cross-terms and thus makes the readability and the understanding of the signal description easier but decreases the time-frequency resolution (the supports of auto-terms are enlarged). The second signal (top right panel) is a mono-component frequency modulation signal with a sinusoidal law. The Wigner-Ville representation (middle right panel) exhibits oscillating terms, induced by the interaction between the different parts of the modulating law. The smoothed Wigner-Ville representation (bottom right panel) reduces the interferences and reveals the signal frequency modulation law.

3.2 Time-frequency representation of ictal patterns

Time-frequency representations are widely used for biomedical signal analysis (19), (49). The applications to ECoG signals were primarily aimed at analyzing (23, 50) and modeling observed signals (51) in epilepsy. However, very few works are related to time-frequency analysis of SEEG signals. In (52), multivariate AR modeling of multichannel SEEG signals combined with adaptive segmentation is used to track rapid dynamic changes in seizure signals for patients with temporal lobe epilepsy.

The main goal is to study the temporal evolution of the frequency contents of SEEG signals during both pre-ictal and interictal periods and to identify reproducible (from a seizure to another) time-frequency signatures, describing qualitatively the various phases of a seizure.

As we do not have *a priori* information which would lead to the choice of a given TFR, various time-frequency representations with fixed kernel were implemented, tested and objectively compared on simulations and on a large real data set (53, 54). The Smoothed Pseudo Wigner-Ville Distribution (SPWVD) which allows two independent smoothing operations in time and in frequency (7), appeared to be well adapted to the representation of the large variety of time frequency patterns revealed from SEEG signals (55). Typically, for smoothing purposes, two Hamming windows with 0,125 s and 0,5 s duration are used respectively for the time and frequency domain smoothing.

Figure 6-a shows the SEEG signal recorded from amygdala during the pre-ictal and ictal period along with its associated SPWVD (Figure 6-b). The electrical onset of this first seizure (S1) occurs at $t = 53$ s and is highlighted by high amplitude spikes. One can notice that chirp-like patterns as well as signatures with nonlinear frequency modulation law and

harmonic structure are revealed by TF analysis during the ictal period. Such patterns are not observed during interictal periods. Of particular interest is the time-frequency signature associated to the tonico-clonic discharge generally invading both mesial and neocortical structures. One can also notice that this signature, occurring around $t = 115$ s and having a multi-component harmonic structure, occurs simultaneously with the first clinical symptoms.

From our database on temporal lobe epilepsies (TLE) (56), we selected SEEG recordings performed in patients candidate to surgery. Using SPWVD, particular SEEG patterns observed in these recordings were reported in (57, 58). An in-depth analysis of the time-frequency plans led us to group these signatures in three classes : transients, elementary modes and mixtures of components :

Transients : These signals have short time support, random or unknown shapes and their time occurrences are unpredictable. They can appear in a SEEG recording in an isolated way or in the form of a repetitive discharge.

1- Isolated transients: they can be short or large (50 ms to 300 ms) with a frequency band going from 5 Hz to 25 Hz. Figure 7-a depicts a large transient followed by short transients. A burst is another example of isolated transients (Figure 7-b). These signals have short time and frequency supports (a time duration of about 0.5 s and a variable central frequency).

2- Transient discharge: it is a succession of transients having a stable or evolutionary nature with regard to their power or their time occurrence. Figure 8 shows a series of transients whose frequency decreases slowly at the beginning, becomes constant afterwards and finally increases; the power of the series decreases at the end.

Another observed situation is that of a series of transients on which oscillatory components superimpose. The example presented on Figure 9 illustrates the first phase of a

change in a signal type where a sequence of spikes is vanishing and a fast rhythmic activity (narrow band signal) is progressively appearing.

Elementary modes: The second class includes the signatures observed on a larger time support but characterized by more structured time-frequency patterns.

1- *Simple mode:* this signature corresponds to a stable and quasi mono-component (rhythm) signal, *i.e.* reproducing the instantaneous frequency of the signal. A pseudo-regular mode corresponds to a quasi-constant frequency (Figure 10-a). An intermittent mode is represented by a mono-component signal with fast changes in the instantaneous frequency (Figure 10-b).

2- *Mixed mode:* a mixed mode is composed of several mono-component signals. Figure 11-a depicts an example of this mode where the signal is composed of a constant frequency and a quasi-linearly decreasing chirp. For the example reported on Figure 11-b, there are various components whose instantaneous frequencies tend to intersect or to move away in the time-frequency plan. A third example presents various components which correspond to the harmonics of a fundamental (Figure 11-c).

Mixtures of components :For these modes, the time-frequency plan is either slightly structured or not structured at all.

1- *Quasi-regular mode:* an example is displayed on Figure 12 where a signature, corresponding to a frequency modulated signal, according to a parabolic law, and a series of transients, can be observed.

2- *"Random" mode:* when the time-frequency plane does not make it possible to qualitatively identify a modulation law governing the signal, one will speak, by misnomer, of a "random" mode. The Figure 13 provides two examples of this class ; the first one

corresponds to a low frequency activity whereas the components of the second one are distributed over a broader frequency band.

On the basis of this qualitative classification, two questions, related to reproducibility, may be stated: i) Can the same signature be found in TFR's of other signals recorded during the same seizure? ii) Is this signature also present in TFR's of signals recorded during other seizures ? To answer these two questions, we selected SEEG recordings performed in a patient suffering from mesial TLE, for the presence of rhythmic sustained discharges of spikes in limbic and neocortical structures from our database. Five seizures (denoted in the following by S1, S2, S3, S4 and S5) were recorded during the pre-surgical evaluation. All recordings (interictal and ictal) were visually analyzed. The seizure pattern was found to be relatively reproducible in analyzed seizures. It can be described as a succession of phases where high amplitude spikes are followed by tonico-clonic discharges in mesial structures (hippocampus and amygdala). Neocortical structures are also affected in seizures, but always secondarily, typically about one minute after initial changes of activity take place in limbic structures. As an important fact, first clinical signs always occur with this secondary discharge. This led us to focus on the TF analysis of SEEG signals recorded from mesial (amygdala, hippocampus) and lateral neocortical (mid temporal gyrus, superior temporal gyrus) structures. We then proposed a detection procedure based on a 2 dimensional time-frequency matched filtering approach (59) : a template defined from the signature (figure 14), was used to evaluate a time-frequency statistics $\eta(t, f)$ in two situations. Situation 1: the template is correlated with TFR's of signals issued from the same seizure (S1). Situation 2: the template is correlated with TFR's of signals recorded during the other seizures (S2 to S5). In the following, results obtained in both situations are detailed. To avoid sensitivity with

respect to signal amplitude variations, the statistics $\eta(t, f)$ is normalized, in the range [0, 1], by dividing correlation values by the local energy of the template and the observed signal.

a) Situation 1. It was first verified that the correlation of the TFR of the signal recorded from the hippocampus with the template (extracted from this same signal) leads to consistent results, as shown in figure 15. When the template reaches the TF zone it was extracted from, statistic η reaches the maximum value of +1.0 and no frequency shift is observed, as illustrated in figure 15-a which displays $\eta(t, 0)$. Results obtained from the correlation of the template with TFR's of other signals of the same seizure are summarized in table 1 which gives the maximum values of the statistics η . High values of η are associated to sharp peaks with no frequency shift, as exemplified in figure 15-b. Detailed analysis of table 1 also shows that the signature is mainly present on signals recorded from mesial (hippocampus, amygdala) and neocortical structures (anterior mid temporal gyrus, superior temporal gyrus). For other signals, only weak peaks are observed.

b) Situation 2. The correlation between the template and TFR's of signals from the four other seizures (S2 to S5) was performed. For S2, no signature similar to the template was present during the ictal period and correlation values remain low. In S3, the signature was found to be present and the template exactly matches it with no translation in frequency. In the two remaining seizures (S4 and S5), a similar signature was present but a frequency shift was necessary for it to be detected. This fact is illustrated in figure 16 which shows the TFR of the hippocampal signal recorded in S4. Visual inspection of this TFR reveals the presence of a signature similar to the template (figure 16-a). However, after correlation with the template, the statistic $\eta(t, 0)$ does not exhibit any dominant sharp peak (figure 16-b). On the other hand, as shown in figure 17, the display of $\eta(t, f)$ (as a function of both time and frequency shifts) now reveals that a sharp peak appears for a frequency shift equal to 0.4 Hz. This shift was found to exist for all TFR's associated to signals retained in the analysis and its

value was found to be constant (0.4 Hz). Similar results were obtained in seizure S5 but with a different frequency shift value of -0.8 Hz estimated also by the frequency position of the peak value in the 2D detection statistics. Results obtained on S4 and S5 demonstrate that a 2D matched filtering improves the detection procedure.

3.3 *Remarks about TFR and signatures detection/classification*

This work can be seen as the first step toward a classification of SEEG time-frequency patterns occurring during temporal epilepsies. A large scale investigation is necessary to achieve such an issue. A similar classification has been recently reported on surface EEG signals recorded in epileptic newborn babies (60). About 3 years ago, Fraszczuk and colleagues (61) presented some results obtained from the application of the matching pursuit algorithm (MPA), initially developed by Mallat and Zhong (62), on signals recorded during mesial temporal seizures. Again, although the method used (MPA) is different from those presented in this study, general results similarly suggest that TF methods are well suited to analyze rapidly changing signals. More recently, the time-frequency content of depth-EEG signals was investigated using spectrogram analysis (63). The authors report that particular signals having a “chirp-like” spectrographic structure are often associated with seizures, confirming previous studies that also pointed up the existence of such TF patterns in epileptic EEG signals. They also present a standard signal processing technique (time matched filtering) that is used for the detection of seizures and for the analysis of their propagation over electrode grids directly placed on neocortical structures. This technique consists in correlating a representative template with spectrograms associated to signals of interest. However, as seen in the previous paragraph, for some patterns visually similar to the chosen template but inside which there exists a shift in frequency (that may be very small), this

detection technique may fail and the two-dimensional matched filtering procedure, by allowing time and frequency shifts, some signatures slightly translated in frequency can be better detected.

4 Conclusion

The change of signal representation domain, when dealing with nonstationary signals as EEG, may lead to a better description of the signal dynamics. Among available approaches, a growing interest for time-scale and time-frequency representations has been noted during the last decade. In this paper, we have presented the theoretical basis of both approaches as well as examples in the field of surface and depth EEG analysis. Both methods share common aspects. Particularly, continuous wavelet transforms allows particular time-frequency representations to be built. However, in this case, the time and frequency resolutions, respectively noted Δt and Δf are interdependent and vary over the time-frequency plane. For the time-frequency representations belonging to the Cohen class, Δt and Δf are constant. Both methods also differ from several aspects. First, the wavelet transforms are linear operators whereas the time-frequency approaches are nonlinear and thus induce interferences between signal components. Second, orthogonal wavelet transforms can efficiently describe signals by means of few coefficients leading to compact representations. This property (not verified in time-frequency representations) may help in some applications where the goal is to compress the information.

In epileptic EEG recordings, these methods appear as an appropriate framework to depict transients signals, structured or unstructured multicomponent patterns with fast changes or slow evolving time-frequency properties. Highly complex seizure patterns can be explored and characterized using such methods Results obtained from experiments conducted in our group are corroborated by results obtained in other studies and demonstrate the benefits one

can expect from nonstationary signal representations. Such a characterization can be further used in localization and classification of seizures (64) (65).

Nonstationary detection procedures may be build in the transformed domain to localize interictal events or particular time-frequency signatures. We found that chirp-like patterns may be observed in TFR's of SEEG signals, as also described in (66). These patterns were found to be identical across different channels of the same seizure recording but were found to slightly vary from one seizure to another. Consequently, one must be cautious with the detection procedure : we demonstrate that a one-dimensional matched filter may fail in detecting patterns visually similar to a searched template and a 2D detection procedure can overcome this limitation. However, from our experience, methods based on matched filtering would not lead to satisfactory results for more significant variations (like strong pattern deformations and superposition of other components). To us, from the signal processing standpoint, new algorithms still have to be designed to deal with more complex deformations of TF patterns (such as affine transformations in both time and frequency or with varying mixtures where some components maybe either suppressed or added). A step in that direction is accomplished in the study reported in (67) where similarities between seizure signals (characterized by their TFR) are automatically extracted using a matching procedure in which both time and frequency deformations are allowed, under minimal cost constraints.

Acknowledgement : The authors wish to thank the three anonymous reviewers for their many constructive comments and Pr P. Chauvel for real data interpretation, performed in the Epilepsy Unit of La Timone Hospital, Marseille, France.

4.1 References

1. Chui CK. Wavelets : a tutorial in theory and applications. Boston: Academic Press; 1992.
2. Chui CK. An introduction to wavelets. Boston: Academic Press; 1992.
3. Chui CK, Montefusco L, Puccio L. Wavelets : theory, algorithms, and applications. San Diego: Academic Press; 1994.
4. Chui CK. Wavelets : a mathematical tool for signal processing. Philadelphia: Society for Industrial and Applied Mathematics; 1997.
5. D'Attellis CE, Fernandez-Berdaguer EM. Wavelet theory and harmonic analysis in applied sciences. Boston: Birkhäuser; 1997.
6. Flandrin P. Temps-Fréquence. Paris: Hermès; 1993.
7. Flandrin P. Time-frequency/time-scale analysis. San Diego: Academic Press; 1999.
8. Foufoula-Georgiou E, Kumar P. Wavelets in geophysics. San Diego: Academic Press; 1994.
9. Hlawatsch F. Time-frequency analysis and synthesis of linear signal spaces : time-frequency filters, signal detection and estimation, and range-Doppler estimation. Boston: Kluwer Academic Publishers; 1998.
10. Mallat SG. A wavelet tour of signal processing. 2nd ed. San Diego: Academic Press; 1999.
11. Motard RL, Joseph B. Wavelet applications in chemical engineering. Boston: Kluwer Academic Publishers; 1994.
12. Ogden RT. Essential wavelets for statistical applications and data analysis. Boston: Birkhauser; 1997.

13. Prasad L, Iyengar SS. Wavelet analysis with applications to image processing. Boca Raton: CRC Press; 1997.
14. Torresani B. Analyse continue par ondelettes. Paris: InterEditions/CNRS; 1995.
15. Wickerhauser MV. Adapted wavelet analysis from theory to software. Wellesley, MA: A.K. Peters; 1994.
16. Cohen A, Ryan RD. Wavelets and multiscale signal processing. London ; New York, N.Y.: Chapman & Hall; 1995.
17. Cohen L. Time-frequency analysis. Englewood Cliffs, N.J: Prentice Hall PTR; 1995.
18. Aldroubi A, Unser MA. Wavelets in biology and medicine. Boca Raton, Fla.: CRC Press; 1996.
19. Akay M, IEEE Engineering in Medicine and Biology Society. Time frequency and wavelets in biomedical signal processing. Piscataway, NJ: IEEE Press; 1998.
20. Binnie CD, Stefan H. Modern electroencephalography: its role in epilepsy management. Clin Neurophysiol 1999;110(10):1671-97.
21. Talairach J, Bancaud J. Stereotaxic exploration and therapy in epilepsy. In: Browns V, editor. Handbook of clinical neurology. The epilepsies. Amsterdam: North Holland; 1974. p. 758-782.
22. Senhadji L, Carrault G, Bellanger JJ, Vignal JP. Multiscale EEG Mapping Of Epileptic Events. In: 13th Annual International Conference of the IEEE Engineering in Medicine and Biology Society; 1991 Oct. 31-Nov. 3; Orlando, FL, USA; 1991. p. 439-440.
23. Zaveri H, Williams WJ, Sackellares JC. Cross time-frequency representation of electrocorticograms in temporal lobe epilepsy. In: 13th Annual International Conference of the IEEE Engineering in Medicine and Biology Society; 1991 Oct. 31-Nov. 3; Orlando, FL, USA; 1991. p. 437-438.

24. Grossmann A, Morlet J. Decomposition of hardy functions into square integrable wavelets of constant shape. *SIAM J Math. Anal.* 1984;15:723-736.
25. Daubechies I. Ten lectures on wavelets. Philadelphia, Pa.: Society for Industrial and Applied Mathematics; 1992.
26. Mallat SG. A theory of multiresolution signal decomposition : the wavelet representation. *IEEE Trans Patt Anal Mach Intell* 1989;31:674-693.
27. Weiss LG. Wavelets and wideband correlation processing. *IEEE Signal Process Mag* 1994;11:13-32.
28. Jaffard S, Meyer Y. Wavelet methods for pointwise regularity and local oscillations of functions. Providence, R.I.: American Mathematical Society; 1996.
29. Mallat SG, Hwang WL. Singularity detection and processing with wavelets. *IEEE Trans Informat. Theory* 1992;38(2):617-643.
30. Senhadji L, Carrault G, Bellanger JJ, Passariello G. Some new applications of the wavelet transforms. In: 14th Annual International Conference of the IEEE Engineering in Medicine and Biology Society; 1992; Paris, France; 1992. p. 2592-2593.
31. Senhadji L, Bellanger JJ, Carrault G. Detection and multi-scales cartography in EEG (in french). In: Meyer Y, Roques S, editors. Progress in wavelet analysis and applications. 3rd international conference on wavelets and applications; 1992 June 8-13; Toulouse, France: Editions Frontieres; 1992. p. 609-614.
32. Senhadji L. Multiresolution approach for nonstationary signal analysis (in french) [PhD.]. [Rennes],: University of Rennes 1; 1993.
33. Senhadji L, Carrault G, Bellanger JJ. Quelques nouvelles applications de la transformée en ondelettes. *Innov. Tech. en Biol. et Méd.* 1993;14:389-403.

34. Senhadji L, Dillenseger JL, Wendling F, Rocha C, Kinie A. Wavelet analysis of EEG for three-dimensional mapping of epileptic events. *Annals of Biomedical Engineering* 1995;23(5):543-552.
35. Senhadji L, Bellanger JJ, Carrault G. Interictal EEG spike detection: a new framework based on wavelet transform. In: *International Symposium on Time-Frequency and Time-Scale Analysis*; 1994 25-28 Oct; Philadelphia, PA, USA; 1994. p. 548-551.
36. Senhadji L, Bellanger JJ, Carrault G. EEG spike detectors based on different decompositions: A comparative study. In: Akay M, editor. *Time-frequency and wavelets in biomedical signal processing*. Piscataway, NJ: IEEE Press; 1998. p. 407-421.
37. Glover JR, Jr., Raghavan N, Ktonas PY, Frost JD, Jr. Context-based automated detection of epileptogenic sharp transients in the EEG: elimination of false positives. *IEEE Trans Biomed Eng* 1989;36(5):519-27.
38. Gotman J, Wang LY. State-dependent spike detection: concepts and preliminary results. *Electroencephalography and Clinical Neurophysiology* 1991;79(1):11-19.
39. Dingle AA, Jones RD, Carroll GJ, Fright WR. A multistage system to detect epileptiform activity in the EEG. *IEEE Trans Biomed Eng* 1993;40(12):1260-8.
40. Ramabhadran B, Frost JD, Jr., Glover JR, Ktonas PY. An automated system for epileptogenic focus localization in the electroencephalogram. *J Clin Neurophysiol* 1999;16(1):59-68.
41. Clark I, Biscay R, Echeverria M, Virues T. Multiresolution decomposition of non-stationary EEG signals: a preliminary study. *Computers in Biology and Medicine* 1995;25(4):373-382.
42. Schiff SJ, Aldroubi A, Unser M, Sato S. Fast wavelet transformation of EEG. *Electroencephalography and Clinical Neurophysiology* 1994;91(6):442-455.

43. D'Attellis CE, Isaacson SI, Sirne RO. Detection of epileptic events in electroencephalograms using wavelet analysis. *Annals of Biomedical Engineering* 1997;25(2):286-293.
44. Goelz H, Jones RD, Bones PJ. Wavelet analysis of transient biomedical signals and its application to detection of epileptiform activity in the EEG. *Clinical EEG (Electroencephalography)* 2000;31(4):181-191.
45. Sartoretto F, Ermani M. Automatic detection of epileptiform activity by single-level wavelet analysis. *Clinical Neurophysiology* 1999;110(2):239-249.
46. Clarencon D, Renaudin M, Gourmelon P, Kerckhoeve A, Caterini R, Boivin E, et al. Real-time spike detection in EEG signals using the wavelet transform and a dedicated digital signal processor card. *Journal of Neuroscience Methods* 1996;70(1):5-14.
47. Jerger KK, Netoff TI, Francis JT, Sauer T, Pecora L, Weinstein SL, et al. Early seizure detection. *J Clin Neurophysiol* 2001;18(3):259-68.
48. Shamsollahi MB, Senhadji L, Le Bouquin-Jeannes R. Représentation temps-fréquence. Théorie et simulations. *Innov. Tech. en Biol. et Méd.* 1998;19(3):123-150.
49. Duchêne J, Senhadji L. Numéros spécial 'Contribution des approches temps-frequence à l'analyse des signaux et des images en génie biomédical'. *Innov. Tech. en Biol. et Méd.* 1998;19(3).
50. Zaveri HP, Williams WJ, Iasemidis LD, Sackellares JC. Time-frequency representation of electrocorticograms in temporal lobe epilepsy. *IEEE Trans Biomed Eng* 1992;39(5):502-9.
51. Bozek-Kuzmicki M, Colella D, Jacyna GM. Feature-based epileptic seizure detection and prediction from ECoG recordings. In: *International Conference on Acoustic Speech and Signal Processing*; 1994; 1994. p. 564-567.

52. Gath I, Feuerstein C, Pham DT, Rondouin G. On the tracking of rapid dynamic changes in seizure EEG. *IEEE Trans Biomed Eng* 1992;39(9):952-8.
53. Shamsollahi MB, Senhadji L, Le Bouquin-Jeannes R. Time-frequency analysis : a comparison of approaches for complex EEG patterns in epileptic seizures. In: 17th Annual Conference Engineering in Medicine and Biology Society; 1995 20-23 Sept.; Montreal, Que., Canada; 1995. p. 1069-1070.
54. Shamsollahi MB. Contribution to time-frequency analysis of electroencephalographic and phonocardiographic signals (in french) [PhD.]. [Rennes],: University of Rennes 1; 1997.
55. Senhadji L, Shamsollahi MB, Le Bouquin-Jeannes R. Representation of SEEG signals using time-frequency signatures. In: Chang HK, Zhang, Y.T, editor. 20th Annual International Conference of the IEEE Engineering in Medicine and Biology Society; 1998; Hong Kong, China; 1998. p. 1454-1457.
56. Bartolomei F, Wendling F, Vignal JP, Kochen S, Bellanger JJ, Badier JM, et al. Seizures of temporal lobe epilepsy: identification of subtypes by coherence analysis using stereo-electro-encephalography. *Clin Neurophysiol* 1999;110(10):1741-54.
57. Shamsollahi MB, Coatrieux JL, Senhadji L, Wendling F, Badier JM. On some time-frequency signatures in stereo-electroencephalography (SEEG). In: Boom H, Robinson, C., Rutten, W., Neuman, M., Wijkstra, H., editor. 18th Annual International Conference of the IEEE Engineering in Medicine and Biology Society; 1996 31 Oct.-3 Nov.; Amsterdam, Netherlands; 1996. p. 1017-1018.
58. Shamsollahi MB, Senhadji L, Le Bouquin-Jeannes R, Chauvel P. Représentation de crise d'épilepsie par des signatures temps-fréquence. *Innov. Tech. en Biol. et Méd.* 1999;20(3):141-150.
59. Shamsollahi MB, Senhadji L, Le Bouquin-Jeannes R. Detection and localization of complex SEEG patterns in epileptic seizures using time-frequency analysis. In: International

Symposium on Time-Frequency and Time-Scale Analysis; 1996 18-21 June; Paris, France; 1996. p. 105-108.

60. Boashash B, Mesbah M. A time frequency approach for newborn seizure detection. *IEEE Eng Med Biol Mag* 2001;20(5):54-64.

61. Franaszczuk PJ, Bergey GK, Durka PJ, Eisenberg HM. Time-frequency analysis using the matching pursuit algorithm applied to seizures originating from the mesial temporal lobe. *Electroencephalogr Clin Neurophysiol* 1998;106(6):513-21.

62. Mallat SG, Zhong S. Matching pursuit with time-frequency dictionaries. *IEEE Trans on Sig. Proc.* 1993;41:3397-3415.

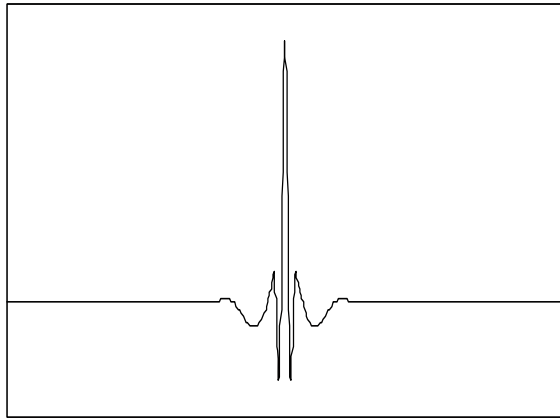
63. Schiff SJ, Colella D, Jacyna GM, Hughes E, Creekmore JW, Marshall A, et al. Brain chirps: spectrographic signatures of epileptic seizures. *Clin Neurophysiol* 2000;111(6):953-8.

64. Park YD, Murro AM, King DW, Gallagher BB, Smith JR, Yaghmai F. The significance of ictal depth EEG patterns in patients with temporal lobe epilepsy. *Electroencephalogr Clin Neurophysiol* 1996;99(5):412-5.

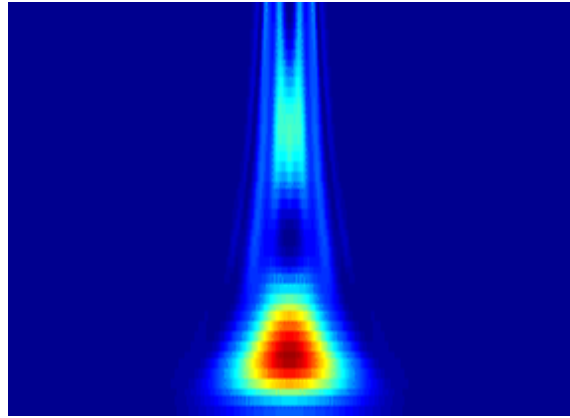
65. Ebersole JS, Pacia SV. Localization of temporal lobe foci by ictal EEG patterns. *Epilepsia* 1996;37(4):386-99.

66. Creekmore JW, Conry J, Colella D, Schiff SJ. Matched-filter based detection and localisation of epileptic seizures from spectrographic chirps in ECoG recordings. In: 17th Annual International Conference of the IEEE Engineering in Medicine and Biology Society; 1995 20-23 Sept.; Montreal, Que., Canada; 1995. p. 517-518.

67. Wendling F, Shamsollahi MB, Badier JM, Bellanger JJ. Time-frequency matching of warped depth-EEG seizure observations. *IEEE Trans Biomed Eng* 1999;46(5):601-5.



a)



b)

Figure 1. a) Time domain representation of the sum of two transients. b) Continuous wavelet representation of the signal in a). The two components are clearly isolated along the scales axis (vertical axis)

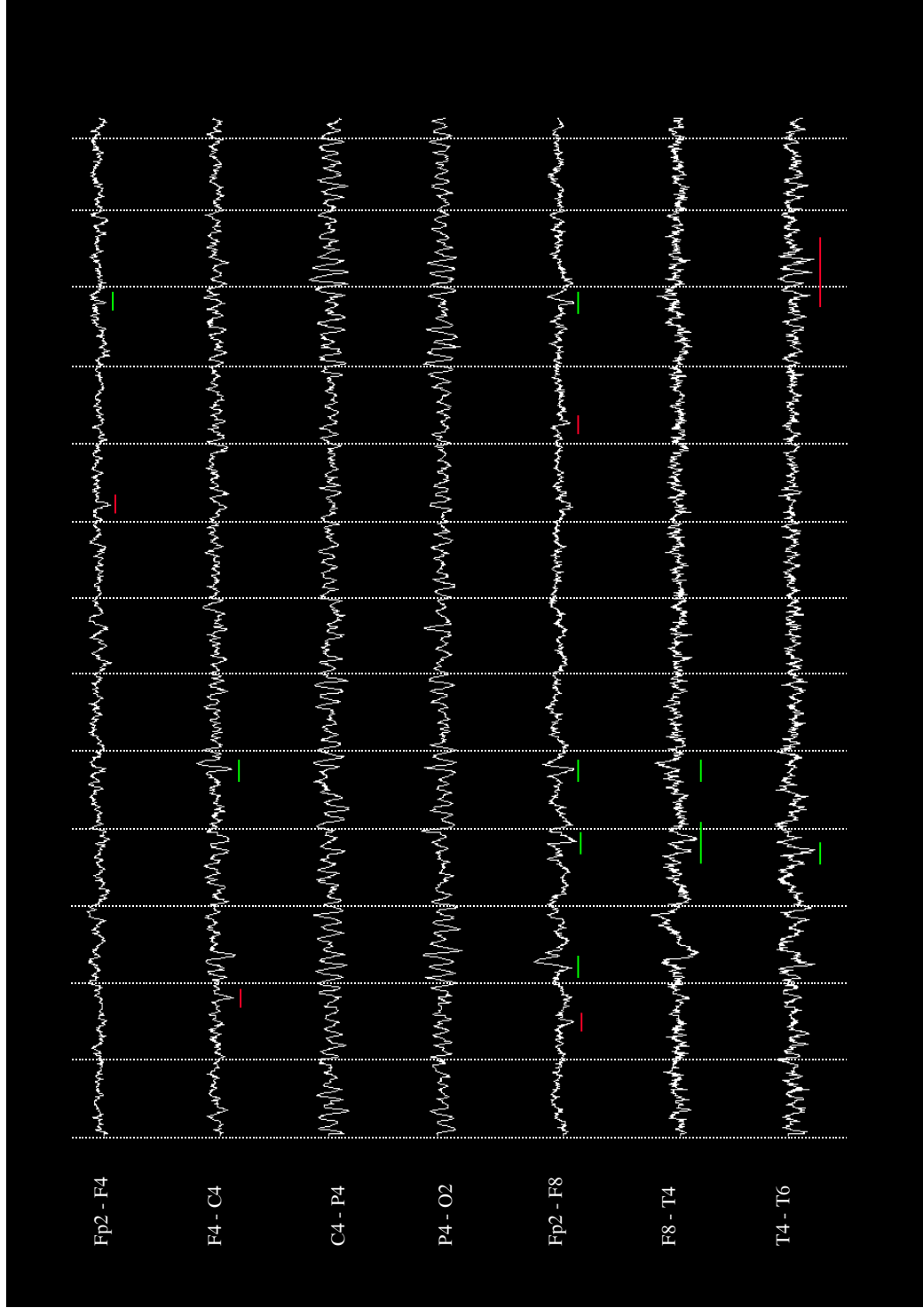


Figure 2. 10 seconds period of a surface EEG recorded during interictal episodes on a patient suffering from a left temporal lobe epilepsy. The signal shows artifact transients (underlined in red), interictal events (underlined in green) activities and various background shapes.

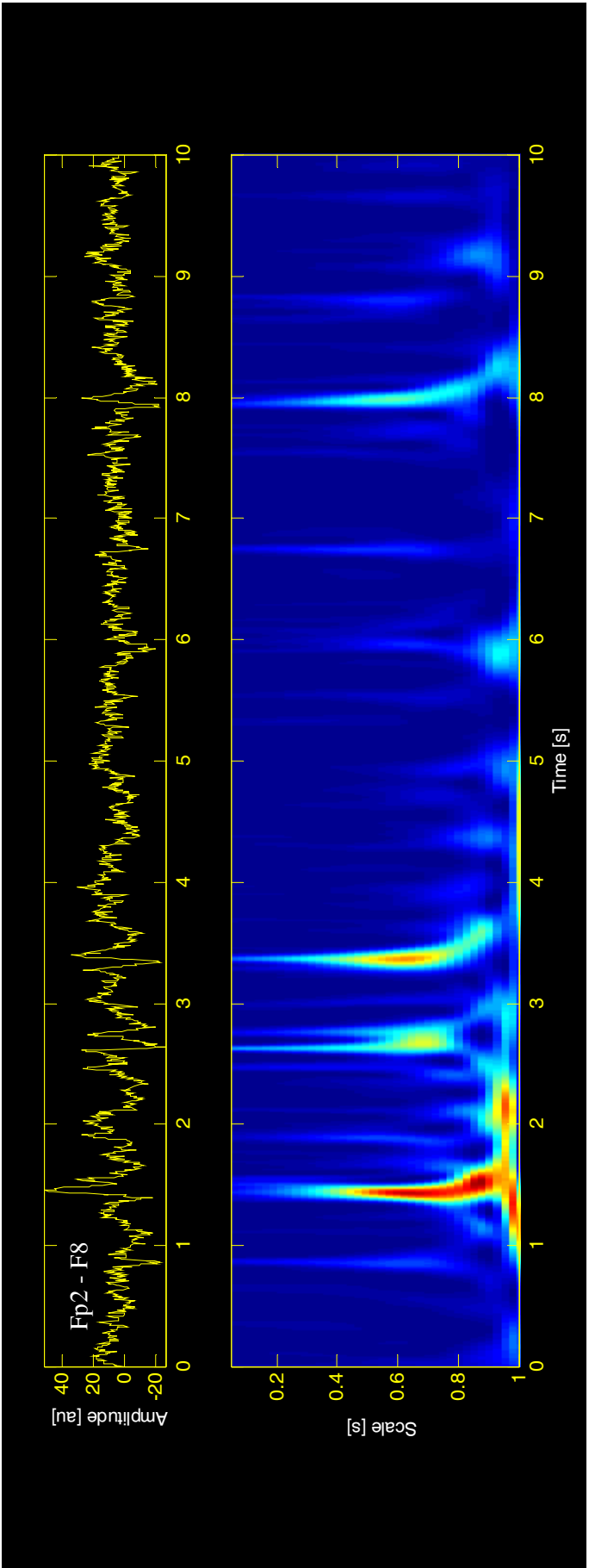


Figure 3. Top panel, 10 second of interictal EEG recording (channel Fp2-F8 of figure 2). Bottom panel, Continuous wavelet transform applied to this signal allows enhancing the epileptic events over a particular range of scaling analysis. Thus interictal event detection may be conducted in the wavelet domain.

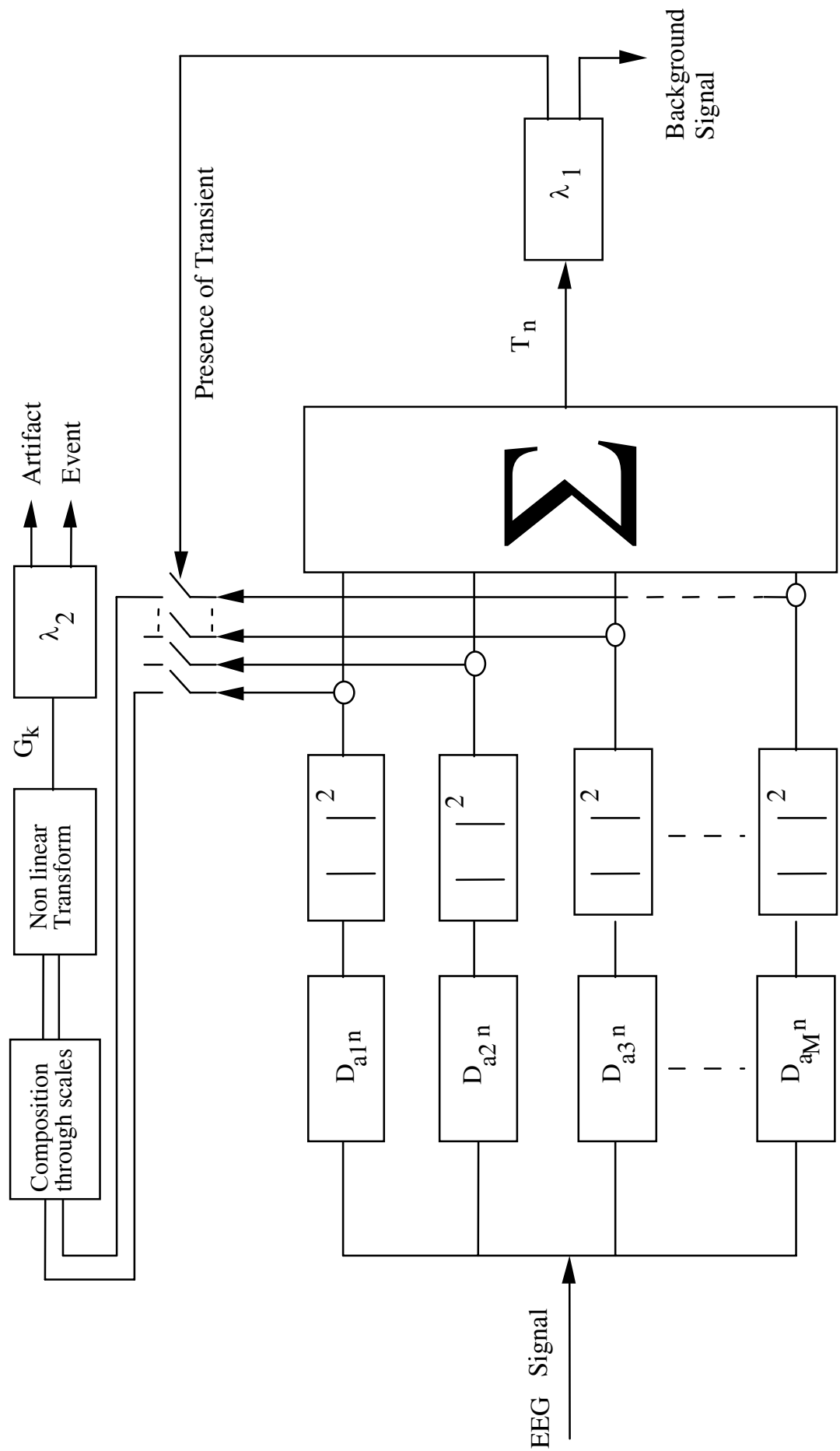


Figure 4. Interictal events detection structure. The signal is decomposed into details using a set M scales. The first threshold allows isolating the transients from the background activity, the second on ensures their classification

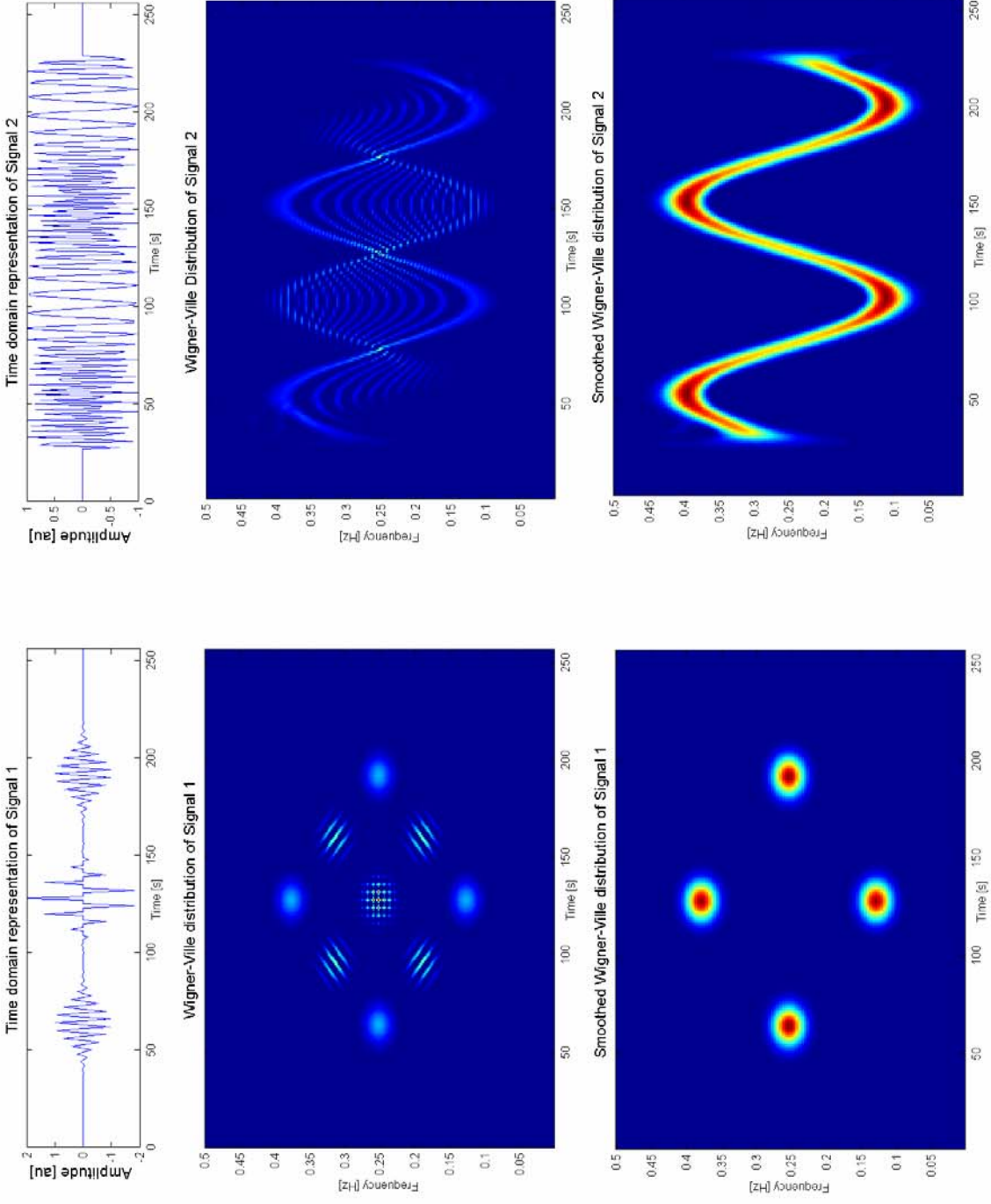


Figure 5. Two examples of TFR on simulated signals. Cross-terms are removed while enlarging the time-frequency supports of auto-terms.

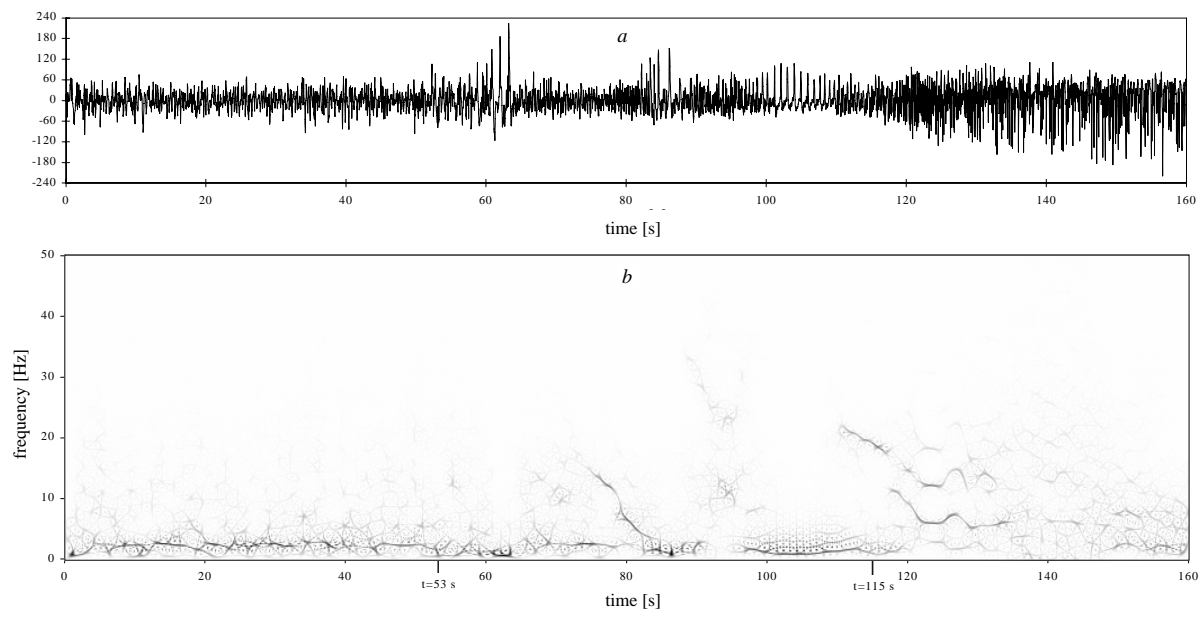


Figure 6. a) Signal recorded from the amygdala during a seizure, b) its SPWVD.

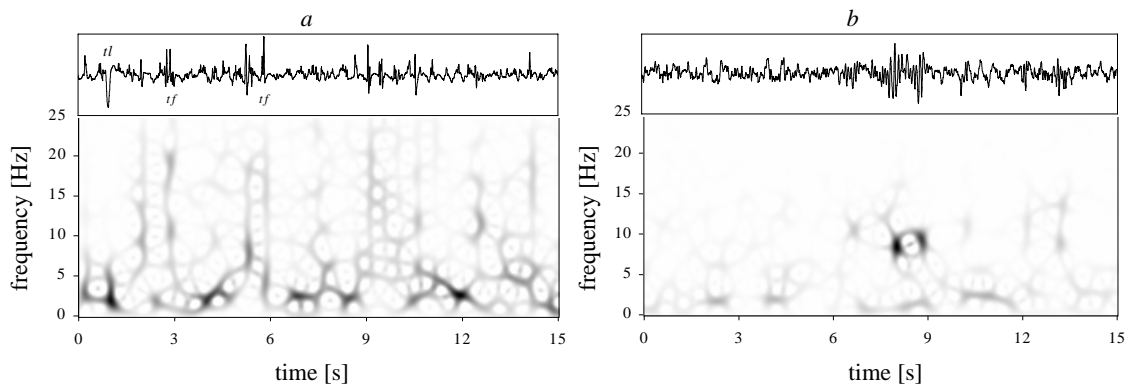


Figure 7. a) Large transients (lt) and short transient (st) occurring in the hippocampus during the interictal period, b) burst occurring in the anterior part of the middle temporal gyrus during the interictal.

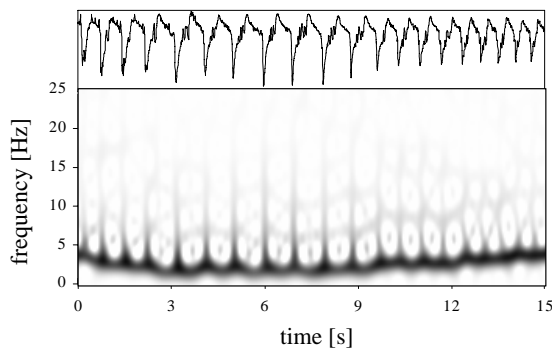


Figure 8. Series of transients appearing in the hippocampus during the ictal period.

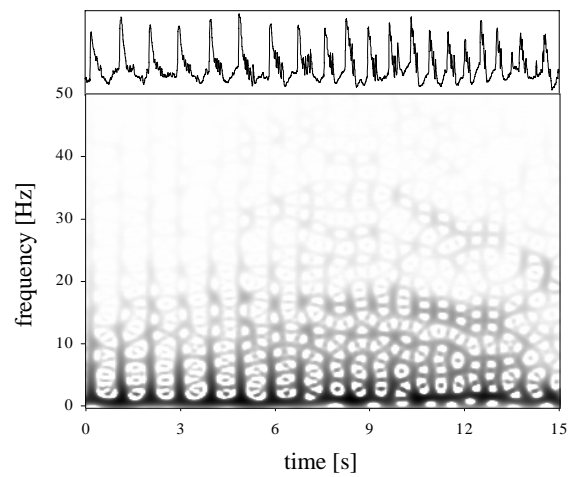


Figure 9. Series of transients followed by oscillations occurring in parahippocampal gyrus during the ictal period.

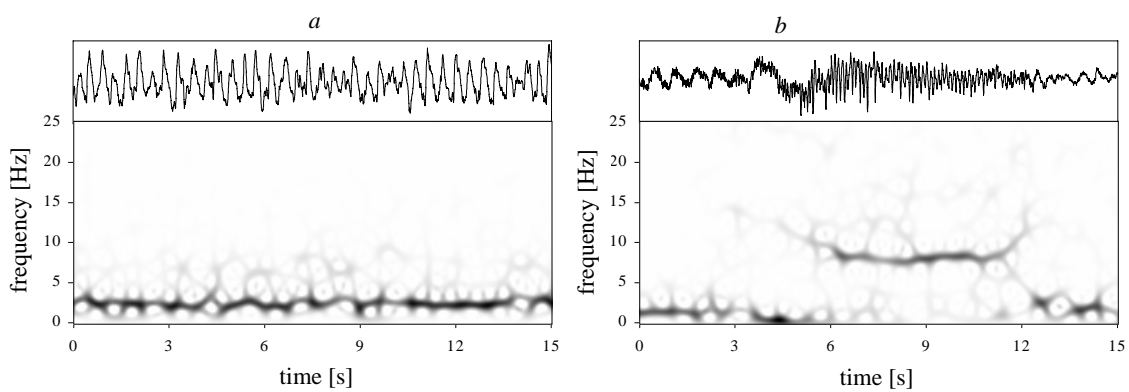


Figure 10. Simple modes: a) pseudo-regular mode recorded from neocortex during the interictal period, b) intermittent mode occurring in parahippocampal gyrus in the ictal period.

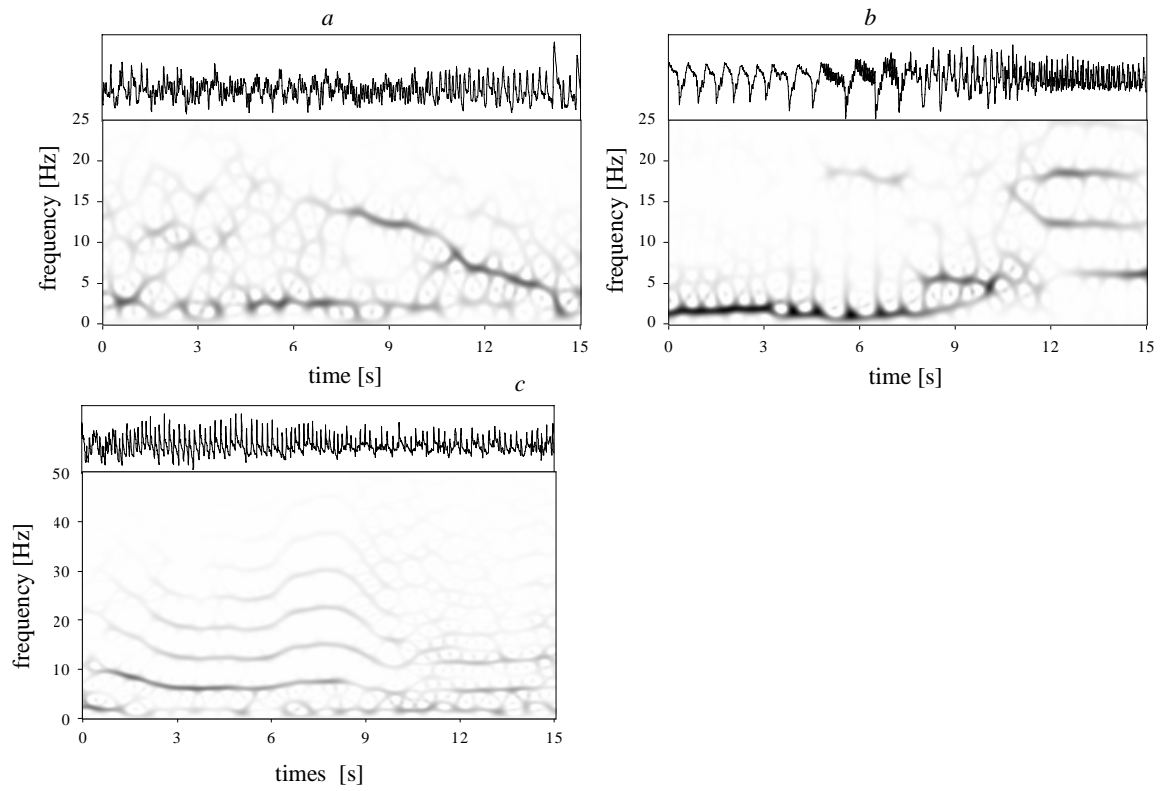


Figure 11. Mixed modes appearing in a) amygdala b) hippocampus and c) parahippocampal gyrus in the ictal period.

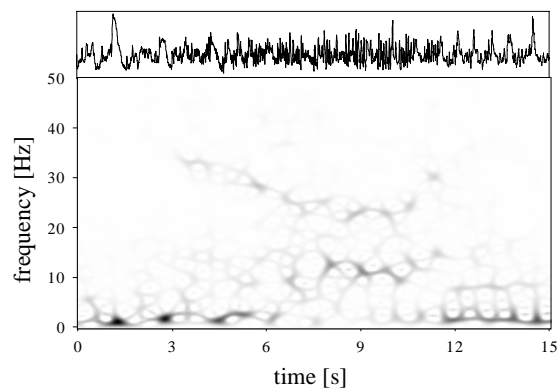


Figure 12. Quasi-regular mixture components mode observed in the amygdala in the ictal period.

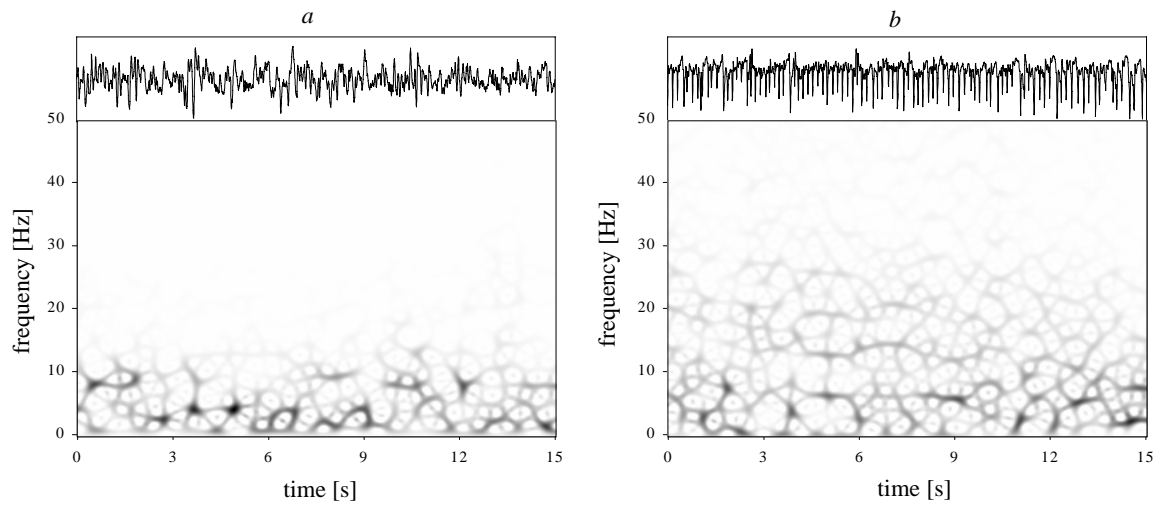


Figure 13. Random components observed in the posterior (a) and anterior (b) parts of the middle temporal gyrus during the interictal period.

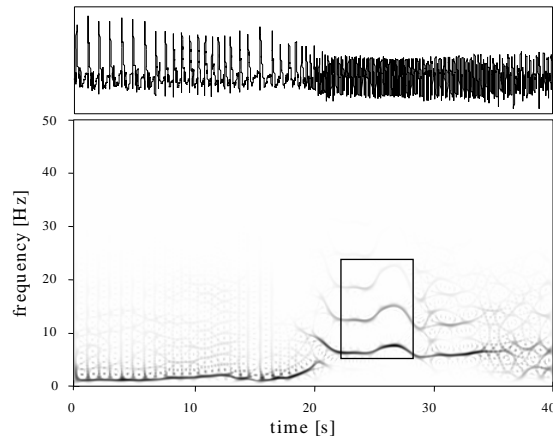


Figure 14. Signal recorded from the hippocampus during a seizure (S1) and its SPWVD. The template selected for use in the detection procedure is bordered by the rectangle.

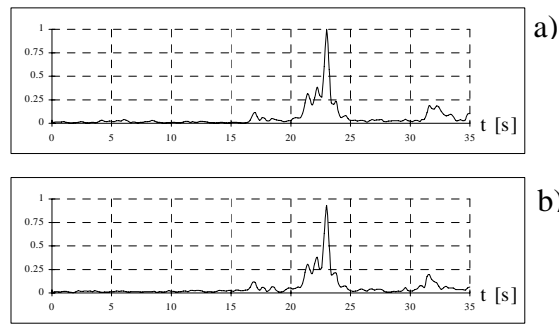


Figure 15. Correlation curves between the template and signals recorded from (a) hippocampus and (b) parahippocampal gyrus during seizure S1. In the first case, the maximum possible correlation value is reached since the template is extracted from the same signal. In the second case, a high value is obtained. This denotes the presence of a similar TF pattern in another cerebral structure, probably signing common underlying mechanism.

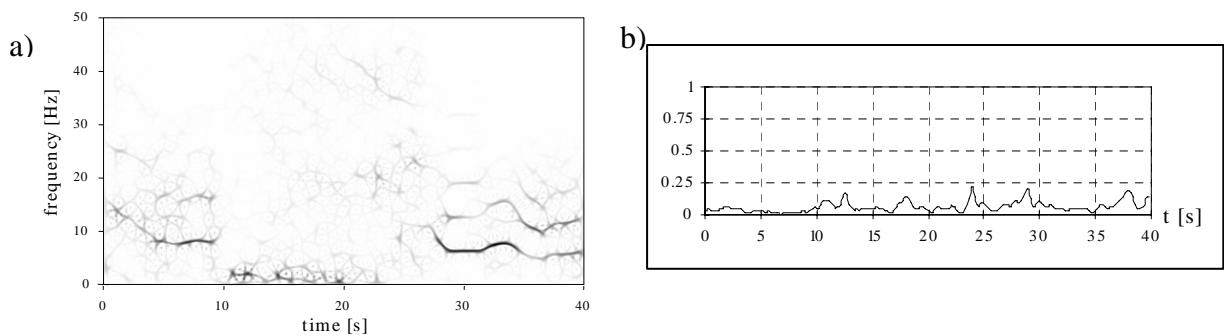


Figure 16. SPWVD of signal recorded from hippocampus during seizure S2 (a) and correlation with the template (b). One can notice that the correlation curve exhibits low values, even if the pattern recorded on signal from the same structure during seizure S2 is visually similar to the template (figure 14). These low values are explained by a slight shift in frequency, not easily detectable by visual inspection.

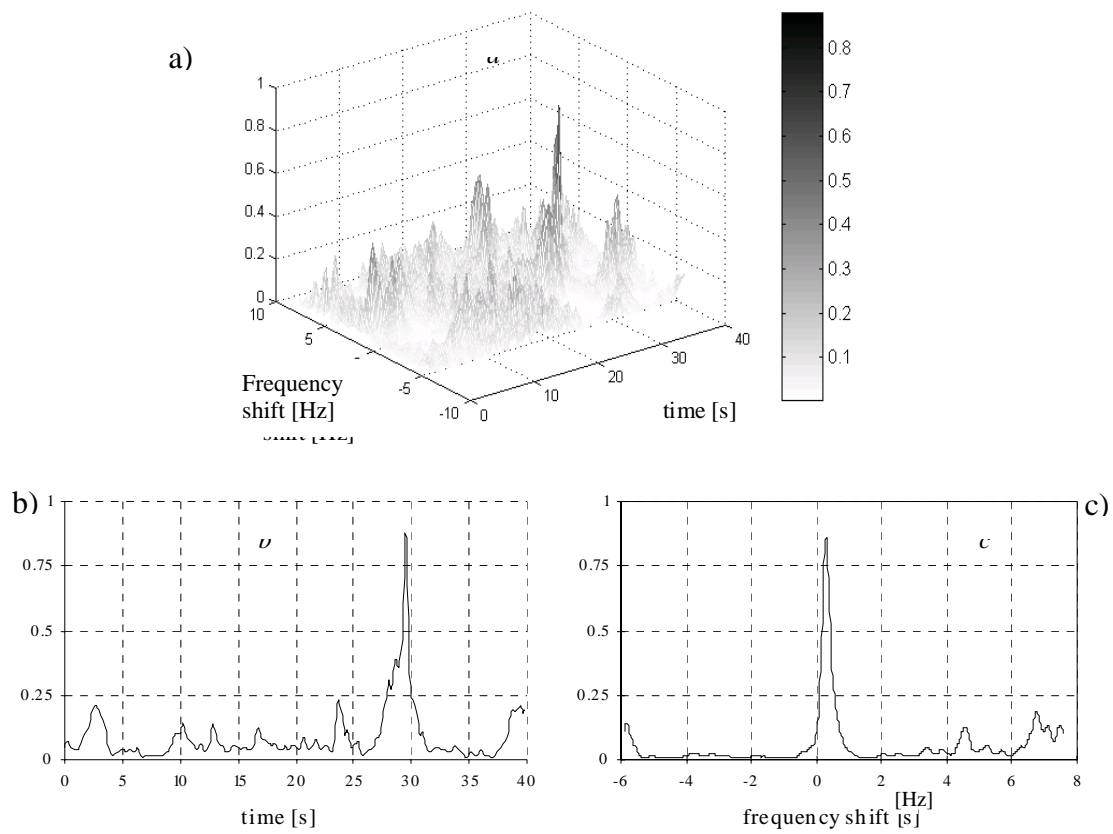


Figure 17. a) 2D correlation between the template (previously extracted from seizure S1) and the signal recorded from the same structure (hippocampus) recorded during seizure S2, b) correlation curve corresponding to a frequency shift of 0.4 Hz, clearly appearing on c) the time slice corresponding to the peak location.

Recorded cerebral structure	Correlation peak
Amygdala	0.8066
Mid Temporal Gyrus (anterior part)	0.6569
Hippocampus	1
Mid Temporal Gyrus (median part)	0.2656
Parahippocampal gyrus	0.7316
Mid Temporal Gyrus (posterior part)	0.2107
Superior Temporal Gyrus (posterior part)	0.7845

Table 1. Maximum values of the correlation between the template and the TFR's of signals recorded from listed cerebral structures.